


Short Note on the Density of States in 3D Weyl Semimetals

K. Ziegler and A. Sinner

Institut für Physik, Universität Augsburg, D-86135 Augsburg, Germany

 (Received 18 May 2018; published 15 October 2018)

The average density of states in a disordered three-dimensional Weyl system is discussed in the case of a continuous distribution of random scattering. Our results clearly indicate that the average density of states does not vanish, reflecting the absence of a critical point for a metal-insulator transition. This calculation supports recent suggestions of an avoided quantum critical point in the disordered three-dimensional Weyl semimetal. However, the effective density of states can be very small such that the saddle-approximation with a vanishing density of states might be valid for practical cases.

DOI: [10.1103/PhysRevLett.121.166401](https://doi.org/10.1103/PhysRevLett.121.166401)

Introduction.—The existence of a metal-insulator transition in disordered three-dimensional (3D) Weyl semimetals has been debated in the recent literature [1–11]. It is closely related to the question, whether or not the average density of states (DOS) at the spectral node vanishes below some critical disorder strength. The self-consistent Born approximation provides such a critical value with a vanishing DOS for weak disorder. It has been argued that rare regions of the random distribution may lead to a non-vanishing average DOS, though [1]. This was supported by recent numerical studies based on the T -matrix approach, which gives an exponentially small DOS [8] but was questioned in a recent study based on an instanton solution [11]. In this short note we show that, depending on the type and strength, a continuous distribution of disorder can create a substantial average DOS at the spectral node in 3D Weyl systems. This requires at least two impurities to create a resonant state between these impurities. A single impurity or a single instanton does not contribute to the spectral weight at the Weyl node, though, in accordance with the arguments in Ref. [11]. This supports the picture of an avoided quantum critical point in the presence of a distribution of impurities, as advocated in Ref. [8].

Model.—The 3D Weyl Hamiltonian for electrons with momentum \vec{p} is expanded in terms of Pauli matrices τ_j ($j = 0, 1, 2, 3$; τ_0 is the 2×2 unit matrix) as $H = H_0 - U\tau_0$, where

$$H_0 = v_F \vec{\tau} \cdot \vec{p} \quad \text{with} \quad \vec{\tau} = (\tau_1, \tau_2, \tau_3). \quad (1)$$

v_F is the Fermi velocity and U is a disorder term, represented by a random potential with mean $\langle U \rangle = E_F$ (Fermi energy) and variance g . The average Hamiltonian $\langle H \rangle = H_0 - E_F \tau_0$ generates a spherical Fermi surface with radius $|E_F|$, and with electrons (holes) for $E_F > 0$ ($E_F < 0$). Physical quantities are expressed in such units that $v_F \hbar = 1$.

The dc limit $\omega \rightarrow 0$ of the conductivity of 3D Weyl fermions depends only on the scattering rate η and the Fermi energy E_F [7]:

$$\sigma(\eta, E_F) = 2 \frac{e^2}{h} \eta^2 \int_0^\lambda \frac{(\eta^2 + k^2)^2 + E_F^2 (2\eta^2 + 2k^2/3 + E_F^2)}{[(\eta^2 - E_F^2 + k^2)^2 + 4\eta^2 E_F^2]^2} \times \frac{k^2 dk}{2\pi^2} \quad (2)$$

with momentum cutoff λ . At the node ($E_F = 0$) the dc conductivity in Eq. (2) is reduced to the expression

$$\begin{aligned} \sigma &= 2 \frac{e^2}{h} \eta^2 \int_0^\lambda \frac{k^2}{(\eta^2 + k^2)^2} \frac{dk}{2\pi^2} \\ &= \frac{e^2 \eta}{2\pi^2 h} \left(\arctan(1/\zeta) - \frac{\zeta}{1 + \zeta^2} \right) \quad (\zeta = \eta/\lambda), \end{aligned} \quad (3)$$

which becomes for $\lambda \gg \eta$

$$\sigma \sim \frac{e^2}{4\pi h} \eta. \quad (4)$$

The last result was also derived by Fradkin some time ago [12]. In contrast to the 2D case, where $\sigma = e^2/\pi h$, the 3D case gives a linearly increasing behavior with respect to the scattering rate.

The results in Eqs. (2)–(4) clearly indicate that a metal-insulator transition in disordered 3D Weyl systems is directly linked to the scattering rate η . The latter describes the broadening of the poles of the one-particle Green's function and is proportional to the average DOS

$$\begin{aligned} \rho_r(E_F) &= \lim_{\epsilon \rightarrow 0} \frac{1}{\pi} \text{Im}[\tilde{G}_{rr}(-i\epsilon)], \\ \tilde{G}(-i\epsilon) &= \langle (H_0 - U\tau_0 - i\epsilon)^{-1} \rangle, \end{aligned} \quad (5)$$

where $\tilde{G}_{\mathbf{r}\mathbf{r}}$ is the diagonal element of \tilde{G} with respect to space coordinates. The self-consistent Born approximation [7,12] at the node $E_F = 0$ reads

$$\eta = \eta I \quad \text{with} \quad I = \gamma[\lambda - \eta \arctan(\lambda/\eta)] \quad (6)$$

for the effective disorder strength $\gamma = g/2\pi^2$. There are two solutions, namely, $\eta = 0$ and a solution with $\eta \neq 0$, which exists only for sufficiently large γ . Moreover, η vanishes continuously as we reduce γ . For $\eta \sim 0$ we obtain the linear behavior

$$\eta \sim \frac{2\lambda}{\pi}(\gamma\lambda - 1), \quad (7)$$

where $\gamma_c = 1/\lambda$ appears as a critical point with $\eta = 0$ for $\gamma \leq \gamma_c$ and $\eta > 0$ for $\gamma > \gamma_c$.

Average density of states.—Few impurities: Lippmann-Schwinger equation. At the node $E_F = 0$ the pure DOS $\rho_{0,\mathbf{r}}(E_F = 0)$ vanishes. However, a few impurities have already a significant effect on the local DOS: Assuming an impurity potential U_N on N sites, we use the identity (lattice version of the Lippmann-Schwinger equation)

$$(G_0^{-1} - U_N)^{-1} = G_0 + G_0(\mathbf{1} - U_N P_N G_0 P_N)^{-1} U_N G_0, \quad (8)$$

where P_N is the projector on the impurity sites and $(\dots)_N^{-1}$ is the inverse on the impurity sites. Although $\rho_{0,\mathbf{r}}(E_F = 0)$ vanishes, the second term on the right-hand side of Eq. (8) can contribute with the poles of $(\mathbf{1} - U_N P_N G_0 P_N)^{-1}$ to the DOS. These poles are ‘‘rare events’’ and require a fine-tuning of the impurity potential, whereas the generic case of a general U_N would still have a vanishing DOS. In a realistic situation the number of impurities is macroscopic with a nonzero density in the infinite system. Then the identity [Eq. (8)] cannot be used for practical calculations

and we have to average over many impurity realizations. This leads to the average Green’s function of Eq. (5), which will be calculated subsequently.

One vs two impurities: The Green’s function G_0 of the system without impurities reads

$$\begin{aligned} G_{0,\mathbf{r}}(-i\epsilon) &= \frac{1}{|\mathcal{B}|} \int_{\mathcal{B}} \frac{e^{i\vec{k}\cdot\mathbf{r}}}{\epsilon^2 + k^2} (i\epsilon\tau_0 + \vec{k} \cdot \vec{\tau}) d^3k \\ &\equiv i\epsilon\gamma_0\tau_0 + \vec{\gamma} \cdot \vec{\tau}, \end{aligned} \quad (9)$$

where \mathcal{B} is the Brillouin zone of the underlying lattice and

$$\begin{aligned} \gamma_0 &= \frac{1}{|\mathcal{B}|} \int_{\mathcal{B}} \frac{e^{i\vec{k}\cdot\mathbf{r}}}{\epsilon^2 + k^2} d^3k, \\ \gamma_j &= \frac{1}{|\mathcal{B}|} \int_{\mathcal{B}} \frac{e^{i\vec{k}\cdot\mathbf{r}} k_j}{\epsilon^2 + k^2} d^3k \quad (j = 1, 2, 3). \end{aligned}$$

Then the diagonal element $G_{0,0} = i\epsilon\gamma_0\tau_0$ vanishes with $\epsilon \sim 0$. This implies that for a single impurity there is no bound state at finite impurity strength $U_{\mathbf{r}}$, since in the impurity term of the Lippmann-Schwinger equation, Eq. (8), the 2×2 matrix

$$(\mathbf{1} - U_{\mathbf{r}} P_{\mathbf{r}} G_0 P_{\mathbf{r}})^{-1} = \frac{1}{1 - i\epsilon\gamma_0 U_{\mathbf{r}}} \tau_0 \quad (10)$$

has a pole at $U_{\mathbf{r}} \sim \infty$. The latter reflects the statement that a potential well in 3D Weyl semimetals never generate spectral density at zero energy [11]. For two impurities, though, there is a resonant intersite bound state between the impurities, since $G_{0,\mathbf{r}-\mathbf{r}'}$ ($\mathbf{r}' \neq \mathbf{r}$) does not vanish for $\epsilon \rightarrow 0$ but decays with a power law for $|\mathbf{r} - \mathbf{r}'|$ due to the Pauli matrix coefficients γ_j in Eq. (9):

$$(\mathbf{1} - U P_{\{\mathbf{r},\mathbf{r}'\}} G_0 P_{\{\mathbf{r},\mathbf{r}'\}})^{-1} = \begin{pmatrix} 1 - i\epsilon\gamma_0 U_{\mathbf{r}} & 0 & -U_{\mathbf{r}}\gamma_3 & -U_{\mathbf{r}}(\gamma_1 - i\gamma_2) \\ 0 & 1 - i\epsilon\gamma_0 U_{\mathbf{r}} & -U_{\mathbf{r}}(\gamma_1 + i\gamma_2) & U_{\mathbf{r}}\gamma_3 \\ U_{\mathbf{r}'}\gamma_3 & U_{\mathbf{r}'}(\gamma_1 - i\gamma_2) & 1 - i\epsilon\gamma_0 U_{\mathbf{r}'} & 0 \\ U_{\mathbf{r}'}(\gamma_1 + i\gamma_2) & -U_{\mathbf{r}'}\gamma_3 & 0 & 1 - i\epsilon\gamma_0 U_{\mathbf{r}'} \end{pmatrix}^{-1}. \quad (11)$$

The degenerate eigenvalues of this matrix

$$\frac{1}{1 - i\epsilon\gamma_0(U_{\mathbf{r}} + U_{\mathbf{r}'})/2 \pm \sqrt{-U_{\mathbf{r}}U_{\mathbf{r}'}(\gamma_1^2 + \gamma_2^2 + \gamma_3^2) - \epsilon^2\gamma_0^2(U_{\mathbf{r}} - U_{\mathbf{r}'})^2/4}} \quad (12)$$

have poles for finite $U_{\mathbf{r}}$, $U_{\mathbf{r}'}$. Thus, the corresponding bound states contribute with a nonvanishing density of states. In the remainder of the Letter this result will be generalized to multiple impurities with corresponding resonant bound states.

Distribution with simple poles: From here on we consider a continuous distribution of the disorder potential U with $\prod_{\mathbf{r}} P(U_{\mathbf{r}}) dU_{\mathbf{r}}$ and average one-particle Green’s function

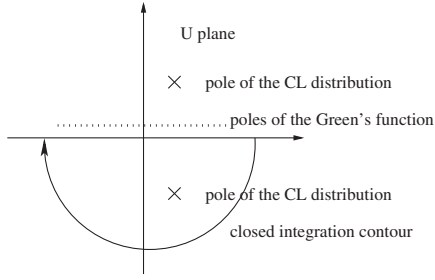


FIG. 1. Poles of the one-particle Green's function and the Cauchy-Lorentz distribution. The contour of the $U_{\mathbf{r}}$ integration encloses only one pole of the Cauchy-Lorentz distribution but not the other poles.

$$\bar{G}(-i\epsilon) = \int (H_0 - U\tau_0 - i\epsilon)^{-1} \prod_{\mathbf{r}} P(U_{\mathbf{r}}) dU_{\mathbf{r}}. \quad (13)$$

For $\epsilon > 0$ the one-particle Green's function $(H_0 - U\tau_0 - i\epsilon)^{-1}$ has poles for $U_{\mathbf{r}}$ on the upper complex half-plane. Assuming that the distribution density $P(U_{\mathbf{r}})$ has isolated poles in the lower complex half-plane, the Cauchy integration can be applied by closing the integration along the real axis in the lower complex half-plane, as depicted in Fig. 1. The simplest realization is the Cauchy-Lorentz distribution

$$P_{\text{CL}}(U_{\mathbf{r}}) = \frac{1}{\pi} \frac{\eta}{(U_{\mathbf{r}} - E_F)^2 + \eta^2}, \quad (14)$$

which gives

$$\bar{G}(-i\epsilon) = [H_0 - (E_F + i\epsilon + i\eta)\tau_0]^{-1}. \quad (15)$$

The average DOS then reads

$$\rho_{\mathbf{r}}(E_F) = \frac{\eta}{\pi} [(H_0 - E_F\tau_0)^2 + \eta^2\tau_0]_{\mathbf{r}\mathbf{r}}^{-1}. \quad (16)$$

The Cauchy-Lorentz distribution has an infinite second moment (i.e., g is infinite). A distribution with a finite second moment can be created from the differential of the Cauchy-Lorentz distribution with respect to η . Many distributions, like the popular Gaussian distribution

$$P_G(U_{\mathbf{r}}) = \frac{1}{\sqrt{\pi g}} e^{-(U_{\mathbf{r}} - E_F)^2/g}, \quad (17)$$

do not have a simple pole structure, though. Then another approach can be applied to show that there is a nonvanishing average DOS.

Distribution without simple poles: Now we only assume that the distribution of $U_{\mathbf{r}}$ is continuous. Then the path of integration can also be deformed away from the poles of the Green's function to obtain a similar result as in the case of simple poles. The calculation would be more complex, though. Therefore, we use a different approach, whose

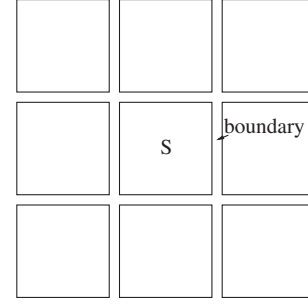


FIG. 2. Dividing the system into cubes $\{S\}$ of size $|S|$ with boundary ∂S .

main idea is to divide the system into cubes $\{S\}$ of finite identical size (cf. Fig. 2). Then we estimate (i) the average DOS inside an isolated cube and (ii) the contribution of the boundary ∂S between the cubes. This approach was used for a periodic lattice [13], for a random tight-binding model with symmetric Hamiltonian [14] and for two-dimensional Dirac fermions with random mass [15]. Later it was applied to a S -wave superconductor with random order parameter [16], and to a D -wave superconductor with random chemical potential [17].

For the average local DOS

$$\bar{\rho}_{\mathbf{r}} = \int \rho_{\mathbf{r}}(U) \prod_{\mathbf{r}} P(U_{\mathbf{r}}) dU_{\mathbf{r}} \quad (18)$$

we obtain from the estimation procedure with steps (i) and (ii) the inequality (cf. Supplemental Material [18])

$$\sum_{\mathbf{r} \in S} \bar{\rho}_{\mathbf{r}} \geq \inf_{\{-a \leq U_{\mathbf{r}}' \leq a\}} \left[\int_{-v}^v \sum_{\mathbf{r} \in S} \rho_{S,\mathbf{r}}(U' + E) dE \times \inf_{\{-v \leq w \leq v\}} \prod_{\mathbf{r} \in S} P(U_{\mathbf{r}}' + w) \right] - \bar{P}_S |\partial S|, \quad (19)$$

where $|S|$ ($|\partial S|$) is the number of sites of S (∂S) and

$$\bar{P}_S = \inf_{\{-a \leq U_{\mathbf{r}}' \leq a\}, -v \leq w \leq v} \prod_{\mathbf{r} \in S} P(U_{\mathbf{r}}' + w).$$

$\bar{P}_S |\partial S|$ is the contribution of the boundary of a cube and the integral is the integrated DOS on a cube S . The boundary term is subtracted because we have removed the boundary. In other words, the left-hand side of Eq. (19) is the average DOS on the entire lattice, the right-hand side is the average DOS on the isolated cube S .

The value of the lower bound requires an adjustment of the still undetermined parameters a and v . The integrated DOS $\int_{-v}^v \sum_{\mathbf{r} \in S} \rho_{S,\mathbf{r}}(U' + E) dE$ on S is the number of eigenvalues on the interval $[-v, v]$ of the S -projected Hamiltonian $H_0 - U'$. The projected Hamiltonian is an $|S| \times |S|$ Hermitian matrix with finite elements, whose eigenvalues are also finite. Thus, for a fixed a we can

choose a sufficiently large v such that all eigenvalues of the projected Hamiltonian are inside the interval $[-v, v]$. In this case the integrated DOS is $|S|$ and we get from Eq. (19) the inequality

$$\sum_{\mathbf{r} \in S} \bar{\rho}_{\mathbf{r}} \geq \bar{P}_S[|S| - |\partial S|]. \quad (20)$$

S can always be chosen such that the size of the cube $|S|$ is larger than the size $|\partial S|$ of its boundary. Then the right-hand side of Eq. (19) is strictly positive. v should not be too large, though, in order to avoid that \bar{P}_S becomes too small, assuming that a typical $P(U_{\mathbf{r}})$ decays for large values. The actual value of \bar{P}_S depends on the distribution and can be exponentially small.

The average DOS of the entire lattice is estimated by the sum over all cubes, normalized by its number N . Since all cubes have the same lower bound, this sum is bounded by the right-hand side of Eq. (20). This indicates that our estimation works only for a macroscopic number of impurities, the case of a single impurity [Eq. (10)] would always give a lower bound zero.

Conclusion.—There is a crucial difference in terms of the average DOS: For a discrete distribution the average DOS is nonzero only if the disorder potential is “resonant” with the pure Green’s function G_0 , according to the second term in Eq. (8). In particular, a single impurity fails to create spectral weight at the Weyl node. On the other hand, for a dense distribution of impurities, represented by a continuous random potential, there is always a nonvanishing average DOS due to interimpurity bound states, provided that the values of $U_{\mathbf{r}}$ cover the entire spectrum of H_0 .

The existence of a critical disorder strength γ_c , as indicated by the self-consistent approximation in Eq. (7), contradicts the existence of a lower nonzero bound of the average DOS in the section “Distribution without simple poles.” Therefore, the self-consistent calculation is not sufficiently accurate to describe the transport properties of the 3D Weyl semimetal properly. Since the lower bound of the average DOS is only a qualitative, although rigorous, estimation, still a reliable approximation is necessary to

obtain an approximative value for the average DOS. The exact result obtained for the Cauchy-Lorentz distribution in the section “Distribution with simple poles” gives only a hint, because this distribution is not generic. A possible option is a $N^{-\alpha}$ expansion with noninteger α [19].

We are grateful to A. Altland for useful discussions. This work was supported by a grant of the Julian Schwinger Foundation.

-
- [1] R. Nandkishore, D. A. Huse, and S. L. Sondhi, *Phys. Rev. B* **89**, 245110 (2014).
 - [2] B. Sbierski, G. Pohl, E. J. Bergholtz, and P. W. Brouwer, *Phys. Rev. Lett.* **113**, 026602 (2014).
 - [3] S. V. Syzranov, V. Gurarie, and L. Radzihovsky, *Phys. Rev. Lett.* **114**, 166601 (2015).
 - [4] J. H. Pixley, D. A. Huse, and S. Das Sarma, *Phys. Rev. X* **6**, 021042 (2016).
 - [5] J. H. Pixley, P. Goswami, and S. Das Sarma, *Phys. Rev. B* **93**, 085103 (2016).
 - [6] J. H. Pixley, D. A. Huse, and S. Das Sarma, *Phys. Rev. B* **94**, 121107(R) (2016).
 - [7] K. Ziegler, *Eur. Phys. J. B* **89**, 268 (2016).
 - [8] J. H. Pixley, Y.-Z. Chou, P. Goswami, D. A. Huse, R. Nandkishore, L. Radzihovsky, and S. Das Sarma, *Phys. Rev. B* **95**, 235101 (2017).
 - [9] B. Sbierski, K. A. Madsen, P. W. Brouwer, and C. Karrasch, *Phys. Rev. B* **96**, 064203 (2017).
 - [10] A. Sinner and K. Ziegler, *Phys. Rev. B* **96**, 165140 (2017).
 - [11] M. Buchhold, S. Diehl, and A. Altland, arXiv:1805.00018.
 - [12] E. Fradkin, *Phys. Rev. B* **33**, 3263 (1986).
 - [13] W. Ledermann, *Proc. R. Soc. London* **182**, 362 (1944).
 - [14] F. Wegner, *Z. Phys. B* **44**, 9 (1981).
 - [15] K. Ziegler, *Nucl. Phys.* **285**, 606 (1987).
 - [16] K. Ziegler, *Commun. Math. Phys.* **120**, 177 (1988).
 - [17] K. Ziegler, M. H. Hettler, and P. J. Hirschfeld, *Phys. Rev. B* **57**, 10825 (1998).
 - [18] See Supplemental Material at <http://link.aps.org/supplemental/10.1103/PhysRevLett.121.166401> for a detailed derivation of the lower bound.
 - [19] K. Ziegler, *Phys. Lett.* **99A**, 19 (1983).